

DISSIPATIVE ADAPTIVE CONTROL FOR STRICT FEEDBACK FORM SYSTEMS

Peter Seiler
Department of Mechanical Engineering
University of California, Berkeley
pseiler@vehicle.me.berkeley.edu

Andrew Alleyne*
Coordinated Science Laboratory
University of Illinois, Urbana-Champaign
alleyne@uiuc.edu

Abstract:

This paper presents a tracking algorithm for the adaptive control of nonlinear dynamic systems represented in Strict Feedback Form with parametric uncertainty. The construction of the stabilizing algorithm is given using Passivity-based arguments that result in an Adaptive Passivity-Based Controller (APBC). The construction of the controller results in a chain of interconnected subsystems with the outputs and inputs of adjacent subsystems sharing a strictly passive relationship. The stability of the overall system is shown via Passivity arguments combined with a modified adaptive algorithm. This is in contrast with other approaches that utilize Lyapunov-based controller designs. This paper also shows a comparison with a controller designed via Adaptive Backstepping with tuning functions, the most popular method for controlling systems of this form. The Adaptive Backstepping Controller (ABC) has many additional coupling terms that make its design and implementation more complex and may also result in unwanted transients. On the other hand, the APBC has a convenient decoupling property that provides a diagnostic tool for detection of non-parametric model error.

Keywords:

Passivity, Nonlinear Control, Strict Feedback Form Systems, Adaptive Control

*Submitted to the European Journal of Control Special Issue on
"Dissipativity of Dynamical Systems: Application in Control"
Dedicated to Vasile Mihai Popov*

Guest Editors : B.D.O. Anderson, P. Kokotovic, I.D.Landau, J.C. Willems

*corresponding author

1. INTRODUCTION

The focus of this paper will be I/O feedback linearizable systems that can be transformed into Strict Feedback Form (Krstic et. al., [13]). Further, these systems will have parametric uncertainty of the following form:

$$\dot{\xi} = f(\xi) + g(\xi)x_1 \quad (1 \text{ a})$$

$$\begin{aligned} \dot{x}_1 &= \theta_1^T f_1(\xi, x_1) + g_1(\xi, x_1)x_2 \\ &\vdots \\ \dot{x}_{r-1} &= \theta_{r-1}^T f_{r-1}(\xi, x_1, \dots, x_{r-1}) + g_{r-1}(\xi, x_1, \dots, x_{r-1})x_r \\ \dot{x}_r &= \theta_r^T f_r(\xi, x_1, \dots, x_r) + g_r(\xi, x_1, \dots, x_r)u \end{aligned} \quad (1 \text{ b})$$

$$y = h(x_1) \quad (1 \text{ c})$$

Here, r denotes the relative degree of the system and $x \in \Re^r$ denotes the portion of the state which is visible through the output equation, (1 c). Equation (1 a) describes the evolution of the state, $\xi \in \Re^{n-r}$, which is not visible at the output. In the following, the system is assumed to be nonlinear minimum phase [10] and therefore the zero dynamics, ξ , are stable. It is assumed that g_i are smooth functions mapping into \Re , $g_i(x)$ are uniformly bounded in x such that $|g_i(x)| \leq G_i \ \forall x$, and $g_i(x) \neq 0 \ \forall x$. The bounds on $g_i(x)$ can be quite large if necessary. The function $h(x_1)$ is a one-to-one smooth invertible map. Furthermore, the f_i are smooth vector fields mapping into \Re^{n_i} . ‘Smooth’ means that the functions are differentiable to any order necessary, potentially C^∞ . The parameter vectors $\theta_i \in \Re^{n_i}$ are unknown constants and an adaptation scheme will be used to estimate them. We assume that bounds on θ_i are known, i.e. we know $M_i \in \Re$ such that $\|\theta_i\| < M_i$. In the following, unless specifically stated, the explicit dependence of f_i and g_i on the system states will be dropped for notational convenience. The form shown in Equation (1) has been previously shown to be reasonable for representing certain types of physical systems with significant actuator dynamics (Alleyne & Hedrick, [1]). In [1], the zero dynamics correspond to the dynamics of the physical

system, a $\frac{1}{4}$ car active suspension, and the r -dimensional dynamics in (1 b) corresponded to those of the electrohydraulic actuator.

Control of systems in the form of Equation (1) has attracted a great deal of interest in the nonlinear controls community. Adaptive Backstepping techniques presented by Kanellakopoulos, et. al. [11] and Kristic and Kokotovic [14] apply an iterative method to develop ‘synthetic inputs’ and estimators for a stabilizing controller. Alvarez-Ramírez, et. al. also use a Backstepping approach to adapt on a more general class of uncertainties, i.e. not just linearly parameterized [4]. [4] presents a nice interpretation of the algorithm as a cascade of PI controllers.

The controller presented in this paper differs significantly from the Backstepping approach by reducing the problem to r simpler problems. The objective is to perform output tracking by creating multiple errors, $e_i = x_i - x_{(i)\text{desired}}$, between the individual states and the desired value of each state [2]. The desired state values are then used as synthetic inputs to control each state error. Notice that the assumption, $g_i(x) \neq 0 \forall x$, ensures that x_{i+1} can always be used to affect x_i . This type of approach using ‘virtual’ control inputs for control design has surfaced previously within the context of the process control industry. Early approaches often were implemented empirically without analytical analysis. These approaches went by the description of ‘cascade’ controllers [17] in the process control industry. This idea was also applied in the analysis of power converters under description of ‘multi-loop’ regulators [15]. For a simple two state example system, the control structure of [17] takes on the structure of a ‘master’ controller and a ‘slave’ controller as shown in Figure 1. The ‘master’ controller sets the desired value of the second state. The ‘slave’ controller then uses the actual control input to track this desired value. In actuality, the ‘master’ and ‘slave’ type of controllers of the Passivity-based algorithm being proposed in the current

work may depend on other states as well as the errors, e_i , in the individual tracking of each state.

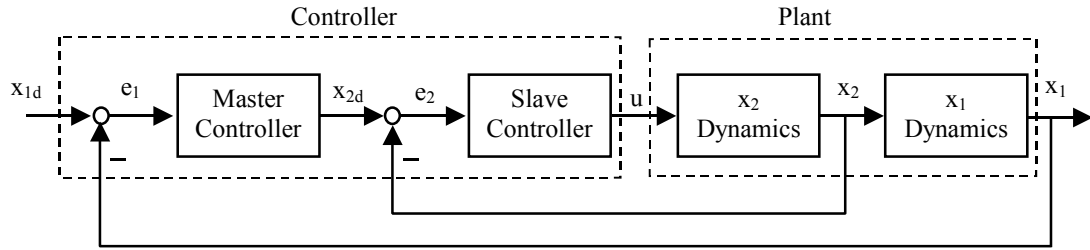


Figure 1: Cascade control interpretation of the design procedure

Conceptually, the chained form of stability given by the control algorithm currently being proposed here can be illustrated in Figure 2.



Figure 2. Sequential Chain of State and Parameter Error Dynamics.

The goal is to have the output of each subsystem passively related to the output of the subsequent subsystem, moving left to right in Figure 2. Having the final, or r -th, subsystem guaranteed to converge to zero assures the eventual convergence of the system output tracking error to zero. In contrast, the Backstepping controllers usually ensure the sum total of all parameter and state errors converge to zero simultaneously. This can be seen conceptually in Figure 3 that shows all state and parameter errors converging along decreasing level sets, $V_n \rightarrow V_{n+1}$, associated with some Lyapunov function.

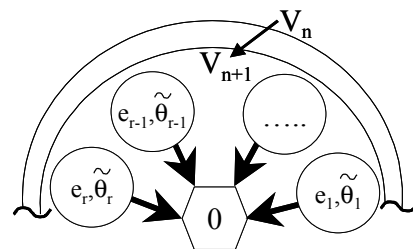


Figure 3. Simultaneous Convergence of all State and Parameter Errors

In the Backstepping approach, a Lyapunov argument is used to show that the derivative of the Lyapunov function of the form $V = \sum_i (e_i^2 + \tilde{\theta}_i^2)$ has a desirable form by considering all errors and parameters simultaneously. Details of the differences between the two approaches will be examined in subsequent sections. However, there are two key benefits to separating the dynamics into multiple errors: (1) the effect of model uncertainty can be localized and (2) differentiation of the system model in the controller can be avoided. The first benefit provides a useful diagnostic tool to locate model uncertainty while the second benefit reduces controller complexity. Both of these benefits are important in the presence of model uncertainty. Previous stability results for this type of control strategy have been obtained for systems in parametric strict feedback form under the assumption of known bounds for the parametric uncertainty (Swaroop et al. [18], Hedrick & Yip [6]).

The remainder of this paper has the following structure: Section 2 describes the Adaptive Passivity-Based Controller design and provides a proof of stability. Section 3 gives a comparison of APBC and an Adaptive Backstepping controller on a simple model. Then Section 4 furthers this comparison by examining the effect of non-parametric model uncertainty, which clarifies the statement that the APBC controller results in decoupled error dynamics. A conclusion then summarizes the main results of this work.

2. ADAPTIVE PASSIVITY-BASED CONTROLLER (APBC) DESIGN

The goal of the APBC is to choose the control, u , such that the output of the system, y , in Equation (1) tracks some desired value. It is assumed that the desired output is bounded, i.e. $y_{\text{desired}} \in L_\infty$. Define the tracking error as:

$$e = y - y_{\text{desired}} \quad (2)$$

For simplicity, assume that $y = h(x_1) = x_1$. By the assumption on h , if $y \neq x_1$ then the function h can always be inverted such that a desired value of x_1 would be determined by $x_{(1)\text{desired}} = h^{-1}(y_{\text{desired}})$. As a generalization of the cascade control idea in Figure 1, define r separate error dynamics as follows:

$$e_i = x_i - x_{(i)\text{desired}} \quad i \in [1, r] \quad (3)$$

where $x_{(i)\text{desired}}$ will be defined shortly. Differentiating each error in Equation (3) gives:

$$\begin{aligned} \dot{e}_i &= \dot{x}_i - \dot{x}_{(i)\text{desired}} = \theta_i^T f_i + g_i x_{i+1} - \dot{x}_{(i)\text{desired}} \quad i \in [1, r-1] \\ \dot{e}_r &= \dot{x}_r - \dot{x}_{(r)\text{desired}} = \theta_r^T f_r + g_r u - \dot{x}_{(r)\text{desired}} \end{aligned} \quad (4)$$

Similar to Green and Hedrick [5], the desired state values, $x_{(i+1)\text{desired}}$, are ‘synthetic inputs’ used to control the i^{th} state for $i = 1, \dots, r-1$. For the r^{th} system, no synthetic input is needed because u enters the e_r dynamics directly. Now the r -dimensional system given by Equation (1 b) has been transformed into ‘ r ’ error systems, each with relative degree = 1. Equation (4) can be rewritten to explicitly show this dependence on the synthetic inputs:

$$\begin{aligned} \dot{e}_i &= \theta_i^T f_i + g_i e_{i+1} + g_i x_{(i+1)\text{desired}} - \dot{x}_{(i)\text{desired}} \quad i \in [1, r-1] \\ \dot{e}_r &= \theta_r^T f_r + g_r u - \dot{x}_{(r)\text{desired}} \end{aligned} \quad (5)$$

The synthetic inputs, $x_{(i+1)\text{desired}}$, are chosen to force their respective error dynamics to decay to zero:

$$\begin{aligned} \overbrace{x_{(i+1)\text{desired}}^{\text{synthetic inputs}}} &\equiv \frac{1}{g_i} \left(-\hat{\theta}_i^T f_i + \dot{x}_{(i)\text{desired}} - k_i e_i \right) \quad i \in [1, r-1] \\ u &\equiv \frac{1}{g_r} \left(-\hat{\theta}_r^T f_r + \dot{x}_{(r)\text{desired}} - k_r e_r \right) \end{aligned} \quad (6)$$

where $\hat{\theta}_i$ is the best estimate of the actual vector θ_i . The justification for the choices in Equation (6) will be given in the proof below. For now, note that this choice tries to cancel most of the dynamics in Equation (5) and replace them with the stabilizing term $-k_i e_i$. Furthermore, the assumption $g_i(x) \neq 0 \forall x$ ensures that (6) is well defined.

Next, the controller is augmented with the following set of estimators:

$$\begin{aligned}\dot{\hat{\theta}}_i &= e_i \Gamma_i f_i - \sigma_i \Gamma_i \hat{\theta}_i \quad i \in [1, r-1] \\ \dot{\hat{\theta}}_r &= e_r \Gamma_r f_r\end{aligned}\tag{7}$$

where Γ_i are $n_i \times n_i$ positive definite matrices which are used to tune the parameter convergence rate. In the simplest form they are diagonal matrices with positive elements which tune each element of the parameter vector estimate, $\hat{\theta}_i$. The gains, σ_i , are scalar functions of $\hat{\theta}_i$ which are used to ensure that parameter errors stay bounded. As will be shown shortly in Equation (9), the error dynamics of Equation (5) reduce to a serial connection of adaptive control systems with the error from the $(i+1)^{th}$ subsystem acting as a disturbance on the i^{th} subsystem. It is well known that bounded disturbances can drive adaptive control systems unstable, so a switching σ -modification [7,8,9,16] is used to improve robustness to this disturbance and ensure error convergence:

$$\sigma_i = \begin{cases} 0 & \|\hat{\theta}_i\| \leq M_i \\ \left(\frac{\|\hat{\theta}_i\|}{M_i} - 1 \right) \cdot |g_i| & M_i < \|\hat{\theta}_i\| \leq 2M_i \\ |g_i| & \|\hat{\theta}_i\| > 2M_i \end{cases}\tag{8}$$

This choice of σ_i uses the known bounds on θ_i to gradually activate the stabilizing term, $-\sigma_i \Gamma_i \hat{\theta}_i$, when $\|\hat{\theta}_i\|$ becomes too large.

The parameter error is defined as $\tilde{\theta}_i = \theta_i - \hat{\theta}_i$. Since it is assumed that θ_i is constant, $\dot{\tilde{\theta}}_i = -\dot{\hat{\theta}}_i$. Combining equations (5)-(7) leads to a chain of interconnected (state and estimator) error dynamics:

$$\begin{aligned}
\dot{\mathbf{e}}_i &= -k_i \mathbf{e}_i + \tilde{\boldsymbol{\theta}}_i^T \mathbf{f}_i + g_i \mathbf{e}_{i+1} & i \in [1, r-1] \\
\dot{\tilde{\boldsymbol{\theta}}}_i &= -\mathbf{e}_i \Gamma_i \mathbf{f}_i + \sigma_i \Gamma_i (\boldsymbol{\theta}_i - \tilde{\boldsymbol{\theta}}_i) & i \in [1, r-1] \\
\dot{\mathbf{e}}_r &= -k_r \mathbf{e}_r + \tilde{\boldsymbol{\theta}}_r^T \mathbf{f}_r \\
\dot{\tilde{\boldsymbol{\theta}}}_r &= -\mathbf{e}_r \Gamma_r \mathbf{f}_r
\end{aligned} \tag{9}$$

Before proceeding, we make note of two assumptions. Here no model uncertainty has been assumed. The interested reader is referred to [3] for the case where this assumption would be relaxed. The theorem below can be modified to make the controller robust against boundable model uncertainty. Secondly it is assumed that $\dot{x}_{(i)\text{desired}}$ is obtained numerically and contains no errors. In actuality, the exact value of $\dot{x}_{(i)\text{desired}}$ is an unknown quantity due to its dependence on $\boldsymbol{\theta}_{i-1}$ (via $\dot{\mathbf{e}}_{i-1}$) which then leads to the use of numerical differentiation. In practice, the approximation of $\dot{x}_{(i)\text{desired}}$ may introduce relevant errors; particularly if the derivative is low-pass filtered. However, since system models usually contain some unknown uncertainty level in practice, the numerical differentiation can oftentimes perform better than an analytical differentiation of a partially unknown model. An alternative to the numerical differentiation is the use of Dynamic Error Filters as shown in [6,18]. If numerical errors are a concern it can be assumed that they be bounded by known values. In other words, if $\dot{\hat{x}}_{(i)\text{desired}}$ is the estimate of the derivative of the synthetic input then $|\dot{x}_{(i)\text{desired}} - \dot{\hat{x}}_{(i)\text{desired}}| \leq \gamma_i$. As a result, the robustness analysis found in [3] can be invoked to compensate for the induced errors and achieve a specified boundary layer performance. With these assumptions, the stability properties of this controller and estimator structure are summarized by the following theorem.

Theorem:

Given the system in Equation (1) and using the synthetic/actual inputs in Equation (6) and the estimators in Equations (7)-(8) with controller gains chosen to be $\{k_i = |g_i| \forall i \in [1, r-1] \text{ and } k_r > 0\}$ and estimator gains given by positive definite matrices Γ_i , the output tracking error $e_l = y - y_{desired}$ is globally asymptotically stable.

Proof: By assumption, g_i is smooth, bounded, and $g_i \neq 0 \forall (x, t)$. Therefore, for any $i \in [1, r-1]$ only two cases have to be considered: $g_i > 0$ and $g_i < 0$. Here the case $g_i > 0 \forall i \in [1, r-1]$ is considered and it is noted that the proof can be easily modified as in [3] if $g_i < 0$ for some i . The proof will proceed in four steps.

Step 1: If $e_{i+1} \in L_2$ then $e_i \in L_2 \quad \forall i \in [1, r-1]$

If $g_i > 0$ the i -th error dynamics can be written as:

$$\begin{aligned}\dot{e}_i &= -|g_i|(e_i - e_{i+1}) + \tilde{\theta}_i^T f_i \quad i \in [1, r-1] \\ \dot{\tilde{\theta}}_i &= -e_i \Gamma_i f_i + \sigma_i \Gamma_i (\theta_i - \tilde{\theta}_i)\end{aligned}\tag{10}$$

This system is output strictly passive [12], which can be verified with the following positive definite storage function:

$$\Phi_i(e_i, \tilde{\theta}_i) = \frac{e_i^2}{2} + \frac{1}{2} \tilde{\theta}_i^T \Gamma_i^{-1} \tilde{\theta}_i \tag{11}$$

Consider $|g_i|e_{i+1}$ as the input and e_i as the only output of the error dynamics given in Equation (10). Differentiating the storage function gives:

$$\begin{aligned}\frac{d}{dt} \Phi_i(e_i, \tilde{\theta}_i) &= \dot{\Phi}_i = e_i \dot{e}_i + \tilde{\theta}_i^T \Gamma_i^{-1} \dot{\tilde{\theta}}_i \\ &= e_i [-|g_i|(e_i - e_{i+1}) + \tilde{\theta}_i^T f_i] + \tilde{\theta}_i^T \Gamma_i^{-1} [-e_i \Gamma_i f_i + \sigma_i \Gamma_i (\theta_i - \tilde{\theta}_i)] \\ &= -|g_i|e_i^2 + e_i |g_i|e_{i+1} + \sigma_i \tilde{\theta}_i^T (\theta_i - \tilde{\theta}_i) \\ &\leq -|g_i|e_i^2 + e_i |g_i|e_{i+1}\end{aligned}\tag{12}$$

The inequality in the final line is a consequence of the following relation:

$$\sigma_i \tilde{\theta}_i^T (\theta_i - \tilde{\theta}_i) = \sigma_i (\theta_i - \hat{\theta}_i)^T \hat{\theta}_i \leq \sigma_i \left(\|\theta_i\| \cdot \|\hat{\theta}_i\| - \|\hat{\theta}_i\|^2 \right) \leq 0 \quad (13)$$

The first inequality in Equation (13) is from the Cauchy-Schwartz Theorem and the second inequality follows from the choice of σ_i in Equation (8). Thus Equation (12) can be rearranged to explicitly demonstrate passivity.

$$\underbrace{e_i}_{\text{output}} \underbrace{|g_i| e_{i+1}}_{\text{input}} \geq \dot{\Phi}_i + \underbrace{|g_i| e_i^2}_{\geq 0} \quad (14)$$

This shows that the error dynamics are output strictly passive, and in fact dissipative, from $|g_i| e_{i+1} \rightarrow e_i$. Since $|g_i|$ is strictly positive, the mapping from $e_{i+1} \rightarrow e_i$ is also output strictly passive. The function $|g_i|$ merely scales the magnitude of the input to a dissipative mapping. Finally, output strictly passive systems are finite gain L_2 stable [12]. Hence $e_{i+1} \in L_2$ implies $e_i \in L_2$ as claimed.

The actual input to each i^{th} subsystem is $|g_i| e_{i+1}$ which necessitates the uniform boundedness assumption on $|g_i|$ in Section 1. To this point, nothing has been proven about $|g_i|$ being bounded. If $|g_i(x)| \rightarrow \infty$, then $|g_i| e_{i+1}$ may not be in L_2 even though $e_{i+1} \in L_2$. In this case, finite gain L_2 stability cannot be used to conclude $e_i \in L_2$. If $|g_i(x)| \in L_\infty$ as assumed then it can still be concluded that $e_i \in L_2$ since $|g_i| e_{i+1} \in L_2$.

Step 2: If $e_{i+1} \in L_\infty$ then $e_i \in L_\infty$ and $\tilde{\theta}_i \in L_\infty \quad \forall i \in [1, r-1]$

The output strict passivity ensures finite gain L_2 stability, but not bounded input bounded output stability. In this step, a Lyapunov-like function is used to prove the boundedness of e_i and $\tilde{\theta}_i$ given $e_{i+1} \in L_\infty$. The positive definite function defined in Equation (11) is used again. Differentiating Φ_i as in Equation (12) yields:

$$\dot{\Phi}_i = -|g_i| e_i^2 + e_i |g_i| e_{i+1} + \sigma_i \tilde{\theta}_i^T (\theta_i - \tilde{\theta}_i) \quad (15)$$

A separate completion of squares for the components of Equation (15)'s right hand side yields two useful inequalities:

$$-\|g_i\|e_i^2 + e_i\|g_i\|e_{i+1} = \frac{\|g_i\|}{2}[-e_i^2 + e_{i+1}^2 - (e_i - e_{i+1})^2] \leq \frac{\|g_i\|}{2}[-e_i^2 + e_{i+1}^2] \quad (16)$$

$$\sigma_i \tilde{\theta}_i^T (\theta_i - \tilde{\theta}_i) = \frac{\sigma_i}{2} \left[-\tilde{\theta}_i^T \tilde{\theta}_i + \theta_i^T \theta_i - (\tilde{\theta}_i - \theta_i)^T (\tilde{\theta}_i - \theta_i) \right] \leq \frac{\sigma_i}{2} [-\tilde{\theta}_i^T \tilde{\theta}_i + \theta_i^T \theta_i] \quad (17)$$

Applying the upper bounds in Equations (16) and (17) to Equation (15):

$$\dot{\Phi}_i \leq \frac{\|g_i\|}{2}[-e_i^2 + e_{i+1}^2] + \frac{\sigma_i}{2}[-\tilde{\theta}_i^T \tilde{\theta}_i + \theta_i^T \theta_i] \quad (18)$$

It remains to be shown that $\dot{\Phi}_i < 0$ outside some compact region in the state space. This is shown conceptually in Figure 4 where the constants will be defined below. Figure 4 represents a 2-dimensional phase plane representation of the state and parameter error space; for the purpose of illustration, $\tilde{\theta}_i$ is shown here as a scalar.

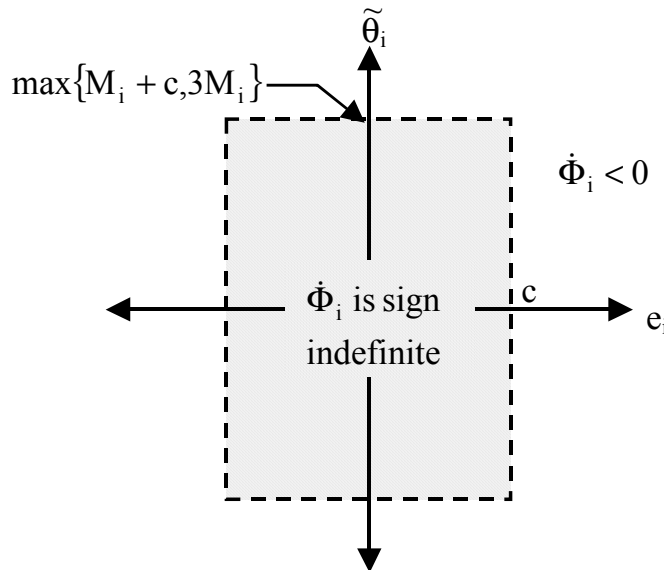


Figure 4: Conceptual view of phase plane

Demonstrating the negative definiteness of $\dot{\Phi}_i$ is accomplished in two stages. First, it can be shown that the second term of Equation (18) is always nonpositive as done in

Equation (13). By assumption on $e_{i+1} \in L_\infty$, there exists a constant, c , such that $|e_{i+1}(t)| < c \ \forall t$. Thus it is clear that $\dot{\Phi}_i < 0$ for $|e_i| > c$. This step forms the vertical walls of the rectangle in the Figure 4.

Second, a close examination of Equation (18) indicates that the first term is sign indefinite if $|e_i| < c$. The purpose of the σ -modification in Equation (8) is to guarantee stability in this case. If $\|\tilde{\theta}_i\| > \max\{M_i + c, 3M_i\}$, then $\dot{\Phi}_i < 0$. $\|\tilde{\theta}_i\| > M_i + c$ ensures that $\tilde{\theta}_i$ is large enough to establish sign definiteness of Equation (18) regardless of e_{i+1} and θ_i . $\|\tilde{\theta}_i\| > 3M_i$ ensures that σ_i is operating at its maximum value of $|g_i|$. Conceptually, this step forms the horizontal walls of the rectangle in the phase plane of Figure 4.

Since $\dot{\Phi}_i < 0$ outside some compact region in the phase plane, there exists a constant $\bar{\Phi}_i > 0$ such that $\dot{\Phi}_i < 0$ for all $\Phi_i > \bar{\Phi}_i$. This implies that Φ_i is bounded and consequently $e_i, \tilde{\theta}_i$ are bounded.

Step 3: $e_r \in L_2 \cap L_\infty$ and $\tilde{\theta}_r \in L_\infty$

Examine the r -th error dynamics:

$$\begin{aligned}\dot{e}_r &= -k_r e_r + \tilde{\theta}_r^T f_r + u^* \\ \dot{\tilde{\theta}}_r &= -\Gamma_r f_r e_r\end{aligned}\tag{19}$$

where u^* is a fictitious input which will be used here only for the analysis. Introduce a storage function similar to Equation (11).

$$\Phi_r(e_r, \tilde{\theta}_r) = \frac{e_r^2}{2} + \frac{1}{2} \tilde{\theta}_r^T \Gamma_r^{-1} \tilde{\theta}_r\tag{20}$$

Differentiate Equation (20) with respect to time.

$$\begin{aligned}\dot{\Phi}_r &= -k_r e_r^2 + e_r u^* \\ \Rightarrow e_r u^* &= \dot{\Phi}_r + k_r e_r^2\end{aligned}\tag{21}$$

Equation (21) shows that, similar to the other $r-1$ error systems, the r -th error dynamics are also output strictly passive and hence finite gain L_2 stable. However, the input to this system is the fictitious input $u^* \equiv 0 \ \forall t$. Clearly, u^* is an L_2 bounded signal and therefore e_r is also L_2 bounded.

Notice that the storage function Φ_r is also a Lyapunov function for the r -th error dynamics. Further, Equation (21) shows that its derivative is negative semidefinite when the fictitious input is zero, $u^* \equiv 0$. Therefore, the pair $(e_r, \tilde{\theta}_r)$ is bounded in time. Thus $e_r \in L_2 \cap L_\infty$ and $\tilde{\theta}_r \in L_\infty$ and the claim is proved.

Step 4: $e_i \in L_2 \cap L_\infty$ and $\tilde{\theta}_i \in L_\infty \ \forall i \in [1, r]$. Moreover $e_1 \rightarrow 0$.

$e_i \in L_2 \cap L_\infty$ and $\tilde{\theta}_i \in L_\infty \ \forall i \in [1, r]$ follows from Steps 1-3 and induction. To prove the asymptotic convergence of e_1 , define $f(t) = e_1^2(t)$. Since $e_1 \in L_2$, $\lim_{T \rightarrow \infty} \int_0^T f(\tau) d\tau$ exists and is finite. Furthermore, $e_1, y_{\text{desired}} \in L_\infty$ imply that $x_1 \in L_\infty$. By the minimum phase assumption, ξ is also bounded, so one can conclude that f_1 and g_1 are bounded. Finally, examining the error dynamics indicates that each term on the right hand side of Equation (22) is bounded.

$$\dot{e}_1 = -|g_1|e_1 + \tilde{\theta}_1^T f_1 + g_1 e_2 \tag{22}$$

Combining all these results, it is straightforward to conclude that \dot{e}_1 is bounded. Consequently, $\dot{f}(t) = 2e_1 \dot{e}_1$ is bounded and thus f is uniformly continuous. By Barbalat's Lemma [12], $f(t) = e_1^2(t) \rightarrow 0$ as $t \rightarrow 0$.



Remarks:

- (1) Strictly speaking, the proof only shows convergence of all intermediate errors, e_i for $i \in [2, r]$, in an L_2 sense: $\lim_{T \rightarrow \infty} \int_T e_i^2(\tau) d\tau = 0$. Mathematically, one could introduce pathological examples whereby the signals converge in an L_2 sense but not to zero; an example of this would be pulses of shrinking width but finite height. However, for many practical types of systems, the previous analysis would indicate that the errors actually converge asymptotically to zero. Thus ‘convergence’ in the remarks below is meant in this L_2 sense with the understanding that asymptotic convergence is typical, though not guaranteed, in practice.
- (2) The Passivity-Based structure of the algorithm dictates a sequential convergence of the tracking errors. The e_r error will converge which causes the e_{r-1} error to converge and so on. All intermediate errors converge which eventually causes the output error to converge. If the i^{th} error (e_i) were non-zero and bounded (e.g. due to model error or disturbances), then one cannot conclude convergence of all subsequent intermediate errors, including the output. The only conclusion, as shown in Step 2 of the proof, is that all intermediate errors will stay bounded. However, this provides a useful tool for detection of non-parametric uncertainty.
- (3) The proof only guarantees that the output and intermediate tracking errors will converge. The parameter errors will remain bounded but may not necessarily converge. For parameter convergence to their true values, we need to impose persistency of excitation constraints. For example, assume the i^{th} error system is zero-state observable [12], i.e. the input and output identically zero implies that the state is identically zero. Then the i^{th} parameter vector, θ_i , will

converge along with the output, e_i . If θ_i is a scalar and $\sigma_i=0$, then zero-state observability of Equation (10) means:

$$e_i, e_{i+1} \equiv 0 \Rightarrow \dot{\tilde{\theta}}_i \equiv 0 \text{ and } \tilde{\theta}_i f_i \equiv 0 \quad (23)$$

To guarantee that $\dot{\tilde{\theta}}_i \equiv 0$ as required for zero-state observability, we need $f_i \neq 0$.

(4) The main benefit of the passivity-based approach is that the controller design problem can be decoupled into r simple problems. This decoupling has two advantages over the Adaptive Backstepping with tuning functions (Krstic et al, [13]): First, the design for each of the decoupled problems is very simple, while the Adaptive Backstepping approach can quickly lead to many terms. Second, the decoupled nature of the APBC is useful for identifying sources of model error. For example, suppose there exists an error in the i^{th} state equation of the model but the rest of the model is accurate. By the analysis in the proof, all errors from e_{i+1} to e_r will converge but the errors from e_1 to e_i may not converge. It will quickly be apparent where the model error exists. In the Adaptive Backstepping approach, the errors and parameter estimators are coupled which makes it difficult to localize model uncertainty. Furthermore, the decoupled nature of the APBC potentially reduces the size of transients. Since the Adaptive Backstepping controller has many coupling terms, model error in one area of the system may lead to large transients in any of the error dynamics.

(5) It was mentioned that the proof would be similar should there be a $g_i < 0$ for some i . If g_i were negative, Equation (16) becomes

$$-|g_i|e_i^2 - e_i|g_i|e_{i+1} = \frac{|g_i|}{2}[-e_i^2 + e_{i+1}^2 - (e_i + e_{i+1})^2] \leq \frac{|g_i|}{2}[-e_i^2 + e_{i+1}^2] \quad (24)$$

The completion of squares is slightly different, but the same upper bound is obtained in (24). The net effect is that the subsequent Equation (18) would be the same for either $g_i < 0$ or $g_i > 0$. Therefore, the proof is valid for either case.

3. COMPARISON OF ADAPTIVE NONLINEAR TECHNIQUES

Consider the following nonlinear plant:

$$\begin{aligned}\dot{x}_1 &= a_1 x_1^3 + x_2 \\ \dot{x}_2 &= a_2 x_2^3 + x_3 \\ \dot{x}_3 &= a_3 x_3 + u \\ y &= x_1\end{aligned}\tag{25}$$

The scalars, a_i , are the unknown plant parameters which have nominal values of $a_1 = a_2 = a_3 = 1.0$. As a result, this three state system is unstable without control and feedback is required. This plant is a simple system that is in Strict Feedback Form with parametric uncertainty as required by Equation (1). For simplicity, the plant under consideration has no zero dynamics and hence it trivially satisfies the nonlinear minimum phase condition. This plant looks quite simple but will provide a suitable comparison between the APBC control and an Adaptive Backstepping Controller (ABC). A setpoint control law will be formulated for this plant with both the APBC and ABC to compare their complexity and performance.

The APBC design of the previous section gives the following synthetic and actual inputs:

$$\begin{aligned}x_{(2)\text{desired}} &= -\hat{a}_1 x_1^3 - k_1 e_1 \\ x_{(3)\text{desired}} &= -\hat{a}_2 x_2^3 + \dot{x}_{(2)\text{desired}} - k_2 e_2 \\ u &= -\hat{a}_3 x_3 + \dot{x}_{(3)\text{desired}} - k_3 e_3\end{aligned}\tag{26}$$

Furthermore, the following set of estimators is obtained via the results of Section 2.

$$\begin{aligned}\dot{\hat{a}}_1 &= \gamma_1 e_1 x_1^3 - \sigma_1 \gamma_1 \hat{a}_1 \\ \dot{\hat{a}}_2 &= \gamma_2 e_2 x_2^3 - \sigma_2 \gamma_2 \hat{a}_2 \\ \dot{\hat{a}}_3 &= \gamma_3 e_3 x_3\end{aligned}\tag{27}$$

The switching- σ law in Equation (8) is used with known bounds on \hat{a}_1 and \hat{a}_2 given by $M_1=M_2=2.0$. Since $g_1=g_2=1$, the Theorem of Section 2 indicates that a choice of gains $k_1=k_2=1.0$ and $k_3>0$ will guarantee convergence of all intermediate errors. For comparison with the Adaptive Backstepping controller, the following gains are used in the simulations: $k_1=k_2=k_3=2.0$. Naturally, the larger gains will only increase the dissipativity between each of the error states $|e_i|$. The estimator gains are chosen as $\gamma_1=\gamma_2=\gamma_3=1.0$. For the setpoint control objective, $y_{\text{desired}}=1.0$. The system given by (25) with controller and estimator given by (26-27) is simulated with a step size of .001 seconds. The initial condition vector is given by $[0.5, 0.8, -0.2]^T$ and the parameter estimates are started at the initial conditions: $[\hat{a}_1(0), \hat{a}_2(0), \hat{a}_3(0)]^T = [1.1, 0.9, 0.9]^T$. Figures 5 and 6 show the tracking and estimator performance of the APBC approach. The upper subplot of Figure 5 shows that the output is converging to the desired setpoint. The middle subplot shows all individual errors are also converging to zero. A closer look at the intermediate errors (lower subplot of Figure 5) shows that e_3 converges first followed by e_2 and then e_1 . This is the sequential convergence dictated by the Passivity-based design: $0 \leftarrow e_3 \leftarrow e_2 \leftarrow e_1$.

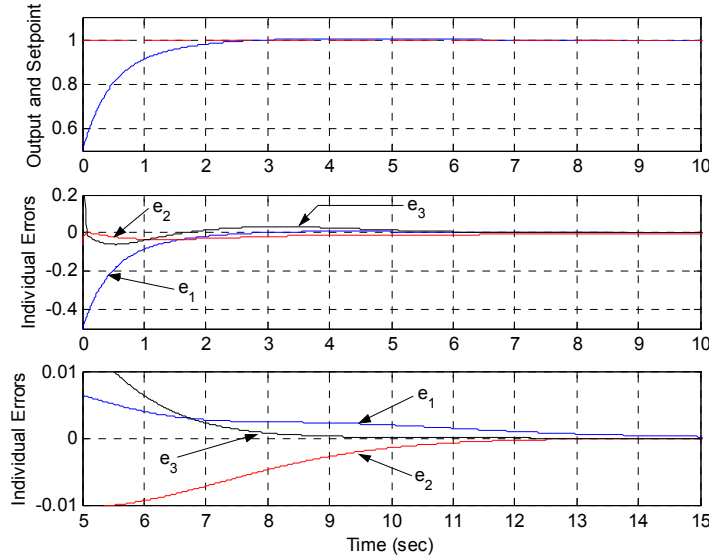


Figure 5: APBC with Perfect Model (Tracking Errors)

Figure 6 shows the parameter estimates are also converging to the true values. In this case, all three error systems satisfy the zero-state observability condition given in Equation (23). Specifically, when $y_{desired} = 1.0$ then $f_i \neq 0$ for $i=1,2,3$ at steady state and thus the parameters should and do converge to the true values.

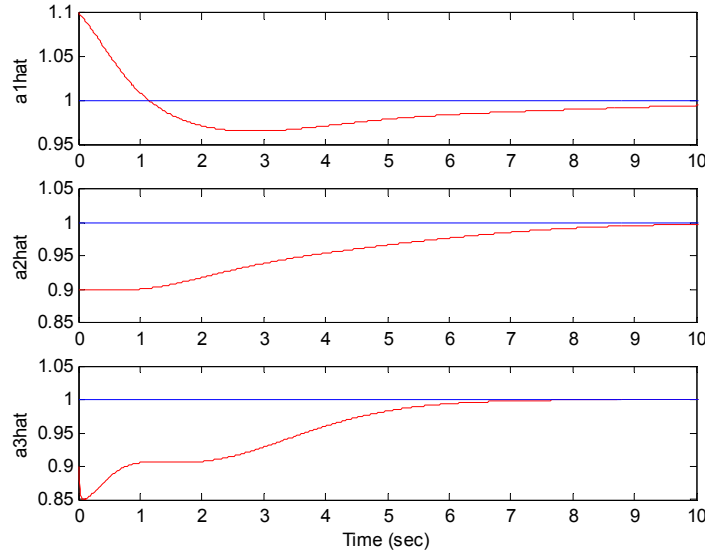


Figure 6: APBC with Perfect Model (Parameter Estimates and True Values)

For comparison a controller is designed using Adaptive Backstepping Control (ABC) with tuning functions as developed in [13,14]. For the same system, this design gives the following synthetic and actual inputs:

$$\begin{aligned}
 x_{(2)desired} &= -\hat{a}_1 x_1^3 - k_1 e_1 \\
 x_{(3)desired} &= -\hat{a}_2 x_2^3 - k_2 e_2 - e_1 + \frac{\partial x_{(2)desired}}{\partial x_1} (x_2 + \hat{a}_1 x_1^3) \\
 &\quad + \frac{\partial x_{(2)desired}}{\partial \hat{a}_1} \gamma_1 x_1^3 \left(e_1 - e_2 - \frac{\partial x_{(2)desired}}{\partial x_1} \right) \\
 u &= -\hat{a}_3 x_3 - k_3 e_3 - e_2 + \frac{\partial x_{(3)desired}}{\partial x_1} (x_2 + \hat{a}_1 x_1^3) \\
 &\quad + \frac{\partial x_{(3)desired}}{\partial x_2} (x_3 + \hat{a}_2 x_2^3) + v_3
 \end{aligned} \tag{28}$$

where v_3 is given by:

$$\begin{aligned}
v_3 = & \gamma_1 \frac{\partial x_{(3)\text{desired}}}{\partial \hat{a}_1} x_1^3 \left(e_1 - e_2 \frac{\partial x_{(2)\text{desired}}}{\partial x_1} - e_3 \frac{\partial x_{(3)\text{desired}}}{\partial x_1} \right) \\
& + \gamma_2 \frac{\partial x_{(3)\text{desired}}}{\partial \hat{a}_2} x_2^3 \left(e_2 - e_3 \frac{\partial x_{(3)\text{desired}}}{\partial x_2} \right) \\
& + \gamma_1 x_1^3 e_2 \frac{\partial x_{(2)\text{desired}}}{\partial \hat{a}_1} \frac{\partial x_{(3)\text{desired}}}{\partial x_1}
\end{aligned} \tag{29}$$

Stabilizing gains for this controller are any $k_i > 0$ and the $\gamma_i > 0$ are the estimator gains. The controller is augmented with the following estimators:

$$\begin{aligned}
\dot{\hat{a}}_1 = & \gamma_1 x_1^3 \left(e_1 - e_2 \frac{\partial x_{(2)\text{desired}}}{\partial x_1} - e_3 \frac{\partial x_{(3)\text{desired}}}{\partial x_1} \right) \\
\dot{\hat{a}}_2 = & \gamma_2 x_2^3 \left(e_2 - e_3 \frac{\partial x_{(3)\text{desired}}}{\partial x_2} \right) \\
\dot{\hat{a}}_3 = & \gamma_3 x_3 e_3
\end{aligned} \tag{30}$$

The partial derivatives contained in Equations (28-30) can be summarized as follows.

$$\begin{aligned}
\frac{\partial x_{(2)\text{desired}}}{\partial x_1} = & -k_1 - 3x_1^2 \hat{a}_1 \\
\frac{\partial x_{(3)\text{desired}}}{\partial x_1} = & (k_1 + 3\hat{a}_1 x_1^2)(-k_2 - \gamma_1 k_1 x_1^6 - 3\gamma_1 \hat{a}_1 x_1^8) - 1 - 3k_1 \hat{a}_1 x_1^2 - 15x_1^4 \hat{a}_1^2 - 6\gamma_1 x_1^5 e_1 \\
& - 6x_1 x_2 \hat{a}_1 - \gamma_1 x_1^6 - 6\gamma_1 k_1 x_1^5 e_2 - 24\gamma_1 x_1^7 \hat{a}_1 e_2 \\
\frac{\partial x_{(3)\text{desired}}}{\partial x_2} = & (-k_2 - 3\hat{a}_2 x_2^2) + (-k_1 - 3x_1^2 \hat{a}_1)(1 + \gamma_1 x_1^6) \\
\frac{\partial x_{(2)\text{desired}}}{\partial \hat{a}_1} = & -x_1^3 \\
\frac{\partial x_{(3)\text{desired}}}{\partial \hat{a}_1} = & x_1^3 (-k_2 - k_1 - \gamma_1 k_1 x_1^6 - 3\gamma_1 \hat{a}_1 x_1^8) - 6x_1^5 \hat{a}_1 - 3x_1^2 x_2 - 3\gamma_1 x_1^8 e_2 \\
\frac{\partial x_{(3)\text{desired}}}{\partial \hat{a}_2} = & -x_2^3
\end{aligned} \tag{31}$$

Equations (28-30) are constructed iteratively from Lyapunov's Direct Method with the following Lyapunov function:

$$V = \frac{1}{2} \tilde{\theta}^T \Gamma^{-1} \tilde{\theta} + \sum_{i=1}^3 \frac{1}{2} e_i^2 \tag{32}$$

where $\tilde{\theta}^T = [\hat{a}_1 \hat{a}_2 \hat{a}_3]$ and $\Gamma = \text{diag}(\gamma_1, \gamma_2, \gamma_3)$. If Equation (32) is differentiated with respect to time along the trajectories of Equation (25) with the ABC given by Equations (28-31), then the Lyapunov function derivative is negative semidefinite.

$$\dot{V} = -\sum_{i=1}^3 k_i e_i^2 \leq 0 \quad (33)$$

Barbalat's lemma can then be applied to conclude that all individual errors converge to zero. Notice that the ABC in Equations (28-31) looks similar to the APBC in Equations (26-27) except that it has additional coupling terms along with terms to calculate $\dot{x}_{(2)\text{desired}}$ and $\dot{x}_{(3)\text{desired}}$. From Equation (31) it is clear that the ABC uses analytically computed derivatives that result in an explosion of terms. Moreover, if an unknown model uncertainty were to exist in one of the state dynamics, it would be very difficult to properly take the partial derivative of it with respect to the states. As a result, the ABC is more complex than the APBC. For example, even for this simple system, the partial $\frac{\partial x_{(3)\text{desired}}}{\partial x_1}$ has 14 terms. Besides complexity, the coupling terms have another drawback. Notice that $x_{(3)\text{desired}}$ and u depend on multiple intermediate errors and parameter estimates in Equations (28) and (29). Moreover, the first and second estimators are coupled to multiple errors in Equation (30). Therefore, if an error occurs in a specific synthetic input or estimator, the error will leak to other synthetic inputs or estimators. This may cause undesired transients and make it difficult to pinpoint which section of the system is causing the error. This idea will be explored further in the comparisons below.

For this comparison, the ABC gains, k_i , are all set equal to 3.0 and the estimator gains are chosen as $\gamma_1 = \gamma_2 = \gamma_3 = 0.1$. These values were chosen to give nominal performance that was similar to the APBC case. In addition, the setpoint and initial conditions were all identical to the APBC case. Figures 7 and 8 show the performance of the ABC under

conditions identical to those in Figs 5 and 6. Specifically, it is clear that all intermediate and output errors converge to zero in Figure 7. What can also be noticed is the non-sequential convergence of the errors that differentiates the ABC from the APBC. Figure 8 shows the parameter estimates along with the nominal values. It appears that \hat{a}_3 is not converging to the true value. The Adaptive Backstepping design only guarantees the boundedness of parameter errors, so the nonconvergence of \hat{a}_3 is not uncommon. The fact that all parameters converged for the APBC is not a general result; it is merely specific to this example where the zero-state observability conditions were satisfied. In summary, despite the variation in algorithm complexity, the performance of the APBC and ABC controllers behave similarly for this case of well-known system dynamics. Any differences in nominal performance can probably be eliminated with further tuning of the appropriate controller.

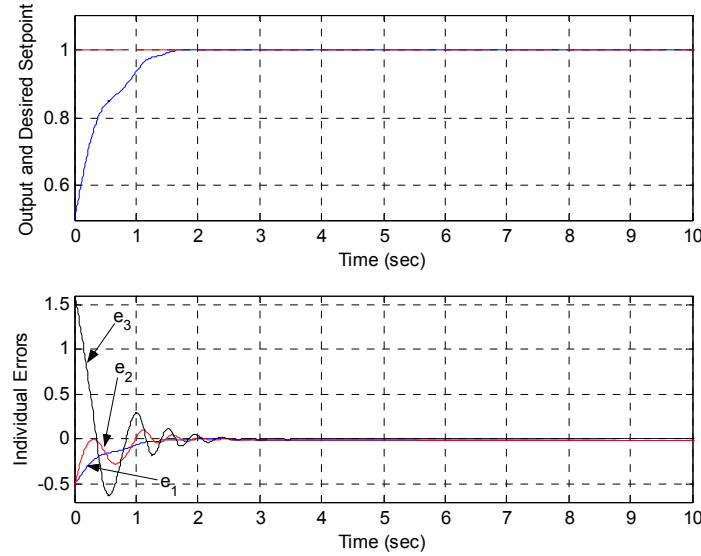


Figure 7: ABC with Perfect Model (Tracking Errors)

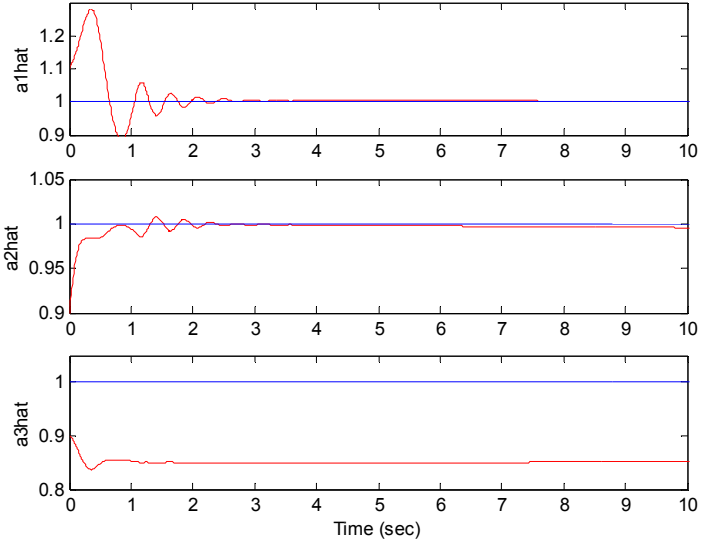


Figure 8: ABC with Perfect Model (Parameter Estimates and True Values)

4. EFFECT OF NON-PARAMETRIC UNCERTAINTY

As shown in Section 3, both the APBC and ABC can handle the case of parametric model uncertainty. In reality, a control designer does not have access to the “true” plant dynamics and must deal with model structure uncertainty. The adaptive control laws are well suited to handle parametric uncertainty, so the actual concern lies in the case of unmodeled dynamics. A controls engineer may wonder if a specific set of dynamical equations models the plant accurately or if neglected dynamics truly are relevant. The real benefit of the APBC approach arises in this case of non-parametric model uncertainty. To simulate the effect of non-parametric model error the previous plant (25) is perturbed by adding a slowly-varying sinusoidal disturbance to the first state equation.

$$\begin{aligned}
 \dot{x}_1 &= a_1 x_1^3 + x_2 + \underbrace{.25 * \sin\left(\frac{2\pi t}{20}\right)}_{\text{non-parametric uncertainty}} \\
 \dot{x}_2 &= a_2 x_2^3 + x_3 \\
 \dot{x}_3 &= a_3 x_3 + u \\
 y &= x_1
 \end{aligned} \tag{34}$$

The time-varying model error will display the error localization property that is a key benefit of APBC design over the ABC. It is assumed that neither controller has knowledge of this additional term in Equation (34). Figure 9 shows the individual errors for both the APBC (upper subplot) and the ABC (lower subplot). Figure 10 shows the parameter estimates for both controller designs. For the APBC, Figure 9 shows the trajectories for e_2 and e_3 converge to zero, while the trajectory for e_1 retains the artifacts of the sinusoidal disturbance. Furthermore, Figure 10 shows that \hat{a}_2 and \hat{a}_3 converge to their true values, but \hat{a}_1 oscillates to compensate for the disturbance. In summary, the disturbance has been localized in the first estimator and error.

Figures 9 and 10 clearly show the decoupling property of the APBC design method. Only those states associated with the uncertain part of the model, along with any states further “up” the passivity chain, manifest an error. This property effectively acts in a controller diagnostic mode and allows the controls engineer to focus attention on improving a specific portion of the system model.

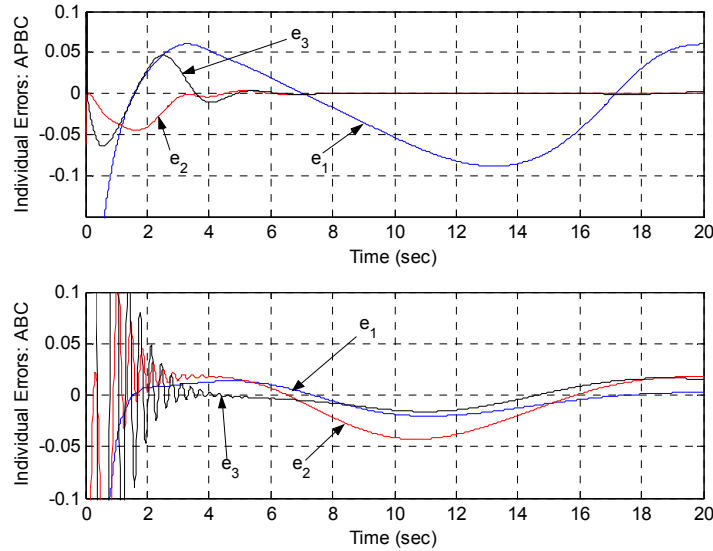


Figure 9: APBC and ABC Individual Errors.

The lower subplot of Figure 9 shows the individual errors for the ABC design. The output error, e_1 , is smaller than the APBC design, but the magnitude is simply a function of the Backstepping gains. The important property of this plot is that all three intermediate errors oscillate similarly about the origin. Furthermore, Figure 10 shows that both \hat{a}_1 and \hat{a}_2 for the ABC design oscillate at the disturbance frequency. The third estimator output, \hat{a}_3 , has a response similar to the perfect model case of Figure 8. This result is explained by Equation (30), which shows that the first two estimators have coupling terms while the third estimator depends only on e_3 and x_3 . The key result of these two figures is that the model uncertainty or disturbance is not localized for the ABC. In fact it has leaked to all the errors and the first two estimators making it impossible to determine the location of the error in the system.

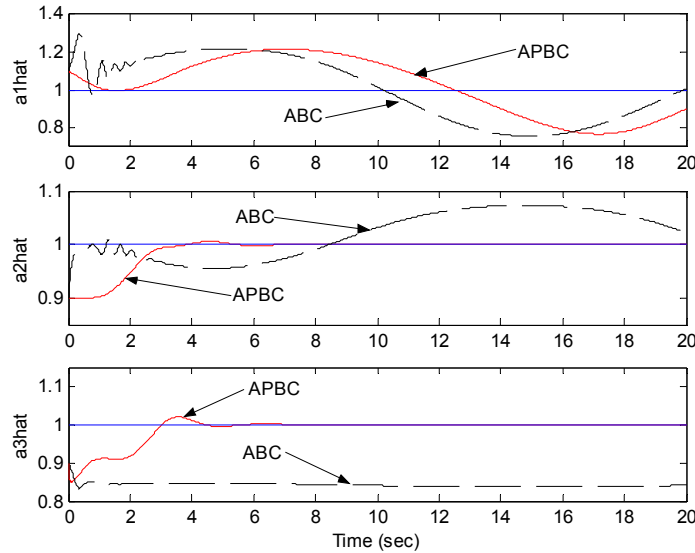


Figure 10: APBC and ABC Parameter Errors.

Finally, as evidence of the potential benefits of the APBC approach, the effect of the Adaptive Backstepping coupling terms on the system transients can be examined. The plant given by Equation (25) is perturbed by adding a constant to the first state equation.

$$\begin{aligned}
 \dot{x}_1 &= a_1 x_1^3 + x_2 + \overbrace{\quad}^{\text{non-parametric uncertainty}} .25 \\
 \dot{x}_2 &= a_2 x_2^3 + x_3 \\
 \dot{x}_3 &= a_3 x_3 + u \\
 y &= x_1
 \end{aligned} \tag{35}$$

Again, this uncertainty is unknown to both the APBC and ABC. As will be shown, all intermediate errors converge to zero for both the APBC and ABC designs. Due to the integrators contained in the parameter estimation algorithms, the estimators for both controllers are able to compensate for this constant disturbance and therefore the outputs still converge to the desired setpoint. It is the transient behavior of the systems that illustrates a difference between the two approaches. Figure 11 shows the synthetic and actual inputs for the nominal system with no model error (25) and the perturbed system (35) when the APBC design is used. These plots show that the synthetic/actual inputs have comparable transients for the nominal and perturbed models (although the steady state values are different to compensate for the model error). For comparison, the ABC was also simulated on the perturbed plant. Figure 12 shows the synthetic and actual inputs for the ABC on the nominal and the perturbed model. The lowest subplot shows that the control effort, u , has very large initial transients on the perturbed plant. Recall from Equations (28) and (29) that this input had the most coupling terms and it is these coupling terms which are resulting in the large transients.

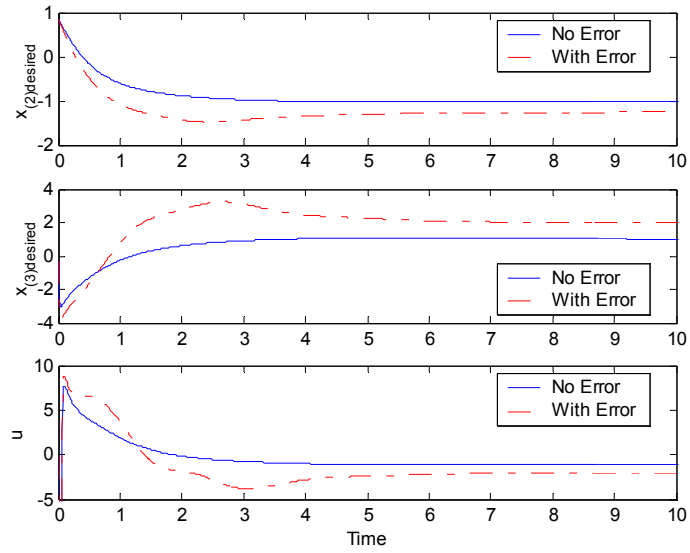


Figure 11: APBC with/without Model Error (Comparison of Synthetic and Actual Inputs)

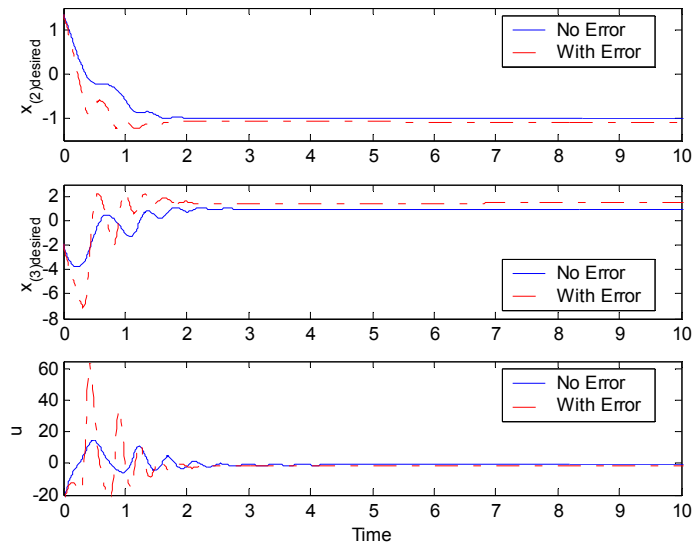


Figure 12: ABC with/without Model Error (Comparison of Synthetic and Actual Inputs)

CONCLUSIONS

In this paper an Adaptive Passivity Based Controller for nonlinear systems in Strict Feedback Form with parametric uncertainty is developed. This design method is then compared against Adaptive Backstepping with tuning functions on a simple 3-state nonlinear model. While the APBC and ABC performance are comparable when the model is perfectly known (other than the parametric error), the APBC offers an easier design procedure. The APBC controller is less complex than the Adaptive Backstepping controller, a fact which may lead to easier implementation. In addition, the APBC design method has a very beneficial decoupling property which can be used as a diagnostic tool to determine where uncertainty lies in the system representation. Finally, when there is non-parametric model uncertainty, the simpler APBC controller may lead to reduced transients in the synthetic and actual inputs.

REFERENCES:

1. Alleyne, A. and Hedrick, J. K., "Nonlinear Adaptive Control of Active Suspensions," *IEEE Transactions on Control Systems Technology*, Vol. 3 No. 1, pp. 94-101, March 1995.
2. Alleyne, A., "Passivity-Based Nonlinear Control Strategies for Strict Feedback Form Systems" *Proceedings of the 1999 ASME IMECE*, DSC Vol. -67, pp. 133-139, Nov. 1999.
3. Alleyne, A., and Liu, R., "Systematic Control of a Class of Nonlinear Systems with Application to Electrohydraulic Cylinder Pressure Control", *IEEE Transactions on Control Systems Technology*, Vol. 8, No. 4, July 2000.
4. Alvarez-Ramírez, J., Suarez, R., and Morales, A., "Cascade control for a class of uncertain nonlinear systems: a backstepping approach", *Chemical Engineering Science*, Vol. 55, No. 16, pp. 3209-3221, August 2000.

5. Green, J. and Hedrick, J.K., "Nonlinear Speed Control for Automotive Engines", *Proceedings of the 1990 ACC*, pp. 2891-2897, San Diego, CA, May 1990.
6. Hedrick, J.K. and Yip, P.P., "Multiple Surface Sliding Control: Theory and Experiment," *ASME Journal of Dynamic Systems, Measurement and Control*, Vol. 122, pp. 586-593, December 2000.
7. Ioannou, P., The Control Handbook, Chapter 54: Model Reference Adaptive Control, pp. 847-858, CRC Press, 1996.
8. Ioannou, P. and Datta, A., "Robust adaptive control: a unified approach", *Proceedings of the IEEE*, Vol. 79, No. 12, pp. 1735-1768, December 1991.
9. Ioannou, P. and Sun, J., Robust Adaptive Control, Prentice Hall, 1996.
10. Isidori, A., Nonlinear Control Systems: An Introduction, Springer Verlag, 1995.
11. Kanellakopoulos, I., Kokotovic, P.V., and Morse, A.S., "Systematic Design of Adaptive Controllers for Feedback Linearizable Systems", *IEEE Transactions on Automatic Control*, Vol. 36, No. 11, pp.1241-1253, November 1991.
12. Khalil, H., Nonlinear Systems, Prentice Hall, 1996.
13. Krstic, M., Kanellakopoulos, I. and Kokotovic, P.V., Nonlinear and Adaptive Control Design, John Wiley and Sons, 1995.
14. Krstic, M. and Kokotovic, P.V., The Control Handbook, Chapter 57.8: Adaptive Nonlinear Control, pp. 980-993, CRC Press, 1996.
15. Middlebrook, R.D., "Topics in multi-loop regulators and current-mode programming", *IEEE Transactions on Power Electronics*, Vol. 2, No. 2, pp.102-124, April 1987.
16. Sastry, S. and Bodson, M., Adaptive Control: Stability, Convergence, and Robustness, Prentice Hall, 1989.

17. Schork, J. and Deshpande, P.B., "Double-cascade controller testbed", *Hydrocarbon Processing*, Vol. 57, No. 6, pp. 113-117, June 1978.
18. Swaroop, D., Hedrick, J.K., Yip, P.P., and Gerdes, J.C., "Dynamic Surface Control for a Class of Nonlinear Systems", *IEEE Transactions on Automatic Control*, Vol. 45, No. 10, pp. 1893-1899, October 2000.